Impaired dopamine release and synaptic plasticity in the striatum of *PINK1*-deficient mice

Tohru Kitada*, Antonio Pisani†, Douglas R. Porter‡, Hiroo Yamaguchi*, Anne Tscherter†, Giuseppina Martella†, Paola Bonsi†, Chen Zhang*, Emmanuel N. Pothos‡, and Jie Shen*§

*Center for Neurologic Diseases, Brigham and Women's Hospital, Program in Neuroscience, Harvard Medical School, Boston, MA 02115; †Department of Neuroscience, University of Rome Tor Vergata and Fondazione Santa Lucia, 00133 Rome, Italy; and ‡Department of Pharmacology and Experimental Therapeutics and Program in Neuroscience, Tufts University School of Medicine, Boston, MA 02111

Edited by Thomas C. Südhof, University of Texas Southwestern Medical Center, Dallas, TX, and approved May 1, 2007 (received for review March 23, 2007)

Parkinson's disease (PD) is characterized by the selective vulnerability of the nigrostriatal dopaminergic circuit. Recently, loss-of-function mutations in the *PTEN-induced kinase 1* (*PINK1*) gene have been linked to early-onset PD. How PINK1 deficiency causes dopaminergic dysfunction and degeneration in PD patients is unknown. Here, we investigate the physiological role of PINK1 in the nigrostriatal dopaminergic circuit through the generation and multidisciplinary analysis of *PINK1*$^{-/-}$ mutant mice. We found that numbers of dopaminergic neurons and levels of striatal dopamine (DA) and DA receptors are unchanged in *PINK1*$^{-/-}$ mice. Amperometric recordings, however, revealed decreases in evoked DA release in striatal slices and reductions in the quantal size and release frequency of catecholamine in dissociated chromaffin cells. Intracellular recordings of striatal medium spiny neurons, the major dopaminergic target, showed specific impairments of corticostriatal long-term potentiation and long-term depression in *PINK1*$^{-/-}$ mice. Consistent with a decrease in evoked DA release, these striatal plasticity impairments could be rescued by either DA receptor agonists or agents that increase DA release, such as amphetamine or L-dopa. These results reveal a critical role for PINK1 in DA release and striatal synaptic plasticity in the nigrostriatal circuit and suggest that altered dopaminergic physiology may be a pathogenic precursor to nigrostriatal degeneration.

neurodegeneration | Parkinson's disease | substantia nigra

Parkinson's disease (PD) is the most common movement disorder and is characterized by bradykinesia, rigidity, resting tremor, and postural instability. These clinical features are thought to result from reduced dopaminergic input to the striatum and the loss of dopaminergic neurons in the pars compacta of the substantia nigra (SNpc). Although the occurrence of PD is largely sporadic, mutations in five distinct genes have been linked to clinical syndromes that are often indistinguishable from sporadic PD. Of these, mutations in the *parkin*, *DJ-1*, and *PINK1* (PTEN induced kinase 1) genes are recessively inherited and include large exonic deletions or frame-shift truncations, suggesting a loss-of-function pathogenic mechanism (1–3).

PINK1 was originally identified as a gene whose transcription was activated by the tumor suppressor PTEN in carcinoma cell lines (4). The *PINK1* gene has eight exons spanning 1.8 kb and encodes 581 aa residues. The deduced amino acid sequence indicates that PINK1 contains a mitochondrial targeting motif (amino acids 1–34) and a kinase domain (amino acids 156–509) that is highly homologous to Ca^{2+}/calmodulin-dependent kinases. Since the first report linking recessively inherited nonsense (W437X) and missense (G309D) mutations in PINK1 to familial PARK6 cases (3), large numbers (>30) of additional truncation and missense mutations have been identified in early-onset PD cases with or without family history (5–11). Genetic analysis revealed that homozygous and compound heterozygous mutations in *PINK1* are highly penetrant and are rather common among early-onset (<50) PD patients and that heterozygous mutations are present among late-onset PD cases at reduced penetrance (6, 7, 10). Patients with PINK1 mutations are often clinically indistinguishable from sporadic PD and generally have good responses to levodopa treatment (6, 10, 12).

How does loss of PINK1 function cause Parkinson's disease? Positron emission tomography (PET) and single-photon emission computed tomography (SPECT) of early-onset PD patients carrying PINK1 mutations revealed presynaptic dopaminergic dysfunction in the striatum, at a level comparable to late-onset idiopathic PD (13–15). These imaging studies have suggested a possible role for PINK1 in the maintenance of normal function and survival of presynaptic dopaminergic terminals in humans. In this study, we investigate how PINK1 deficiency leads to PD and whether loss of PINK1 function in mice causes dopaminergic dysfunction.

Results

Generation of *PINK1*$^{-/-}$ Mice. To generate a mutant mouse that lacks PINK1, we chose to create a targeted germ-line deletion of exons 4–7 (Fig. 1*A*). The deletion of exons 4–7 removes the majority of the kinase domain and creates a nonsense mutation at the beginning of exon 8 because of a shift of the reading frame. The truncated mRNA from the targeted allele is likely to be degraded through nonsense-mediated decay. The linearized targeting vector was transfected into ES cells, and 350 ES clones were screened by Southern blot analysis using the 3′ external probe for the presence of the expected 6.9-kb fragment, which represents the targeted allele (Fig. 1*B*). Four positive clones were then tested by PCR using primers 3 and 4 to confirm the correct recombination in the 5′ homologous region. Two ES clones were injected into blastocytes to generate chimeric mice, which were bred to obtain F_1 heterozygous mutant mice. F_2 homozygous mutant mice were confirmed by Southern blot analysis using a probe specific for the *PGK-Neo* cassette and the 3′ probe and by PCR using primers 3 and 4, followed by sequencing. Northern blot analysis using a probe specific for exon 8 showed the absence and a reduction of *PINK1* mRNA in the brain of homozygous and heterozygous mutant mice, respectively, confirming that truncated *PINK1* transcripts containing exons 1–3 and 8 are

Author contributions: A.P., E.N.P., and J.S. designed research; T.K., D.R.P., H.Y., A.T., G.M., P.B., and C.Z. performed research; T.K., A.P., H.Y., C.Z., E.N.P., and J.S. analyzed data; and A.P., E.N.P., and J.S. wrote the paper.

The authors declare no conflict of interest.

This article is a PNAS Direct Submission.

Freely available online through the PNAS open access option.

Abbreviations: DA, dopamine; EPSC, excitatory postsynaptic current; HFS, high-frequency stimulation; LTD, long-term depression; LTP, long-term potentiation; MS, medium-sized spiny; PD, Parkinson's disease; SNpc, pars compacta of the substantia nigra; TH, tyrosine hydroxylase.

§To whom correspondence should be addressed at: Center for Neurologic Diseases, Brigham and Women's Hospital, Program in Neuroscience, Harvard Medical School, New Research Building, Room 636E, 77 Avenue Louis Pasteur, Boston, MA 02115. E-mail: jshen@rics.bwh.harvard.edu.

This article contains supporting information online at www.pnas.org/cgi/content/full/0702717104/DC1.

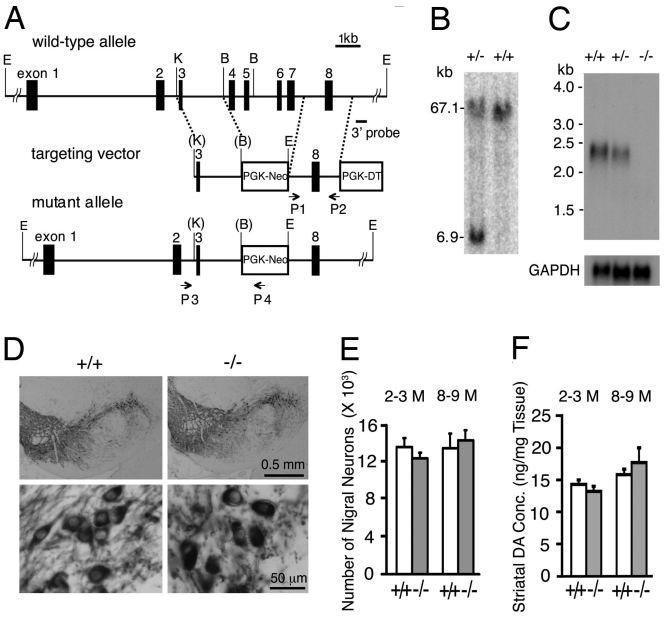

Fig. 1. Normal dopaminergic neurons and DA levels in *PINK1*$^{-/-}$ mice. (*A*) Targeting strategy. The KpnI (K)-Bsr GI (B) fragment containing exon 3 is used as the 5′ homologous region. P1 and P2 represent the positions of the primers used to amplify the 3′ homologous region that contains exon 8. The 3′ probe indicates the position of the 3′ external probe used to screen for targeted ES cells carrying the proper recombination in the 3′ homologous region. P3 and P4 are the primers used to confirm the correct recombination in the 5′ homologous region. E, EcoRV; K, KpnI; B, Bsr GI. (*B*) Southern blot analysis of ES cells by using the 3′ probe. The 67.1-kb EcoRV fragment represents the wild-type allele, whereas the 6.9-kb EcoRV fragment represents the targeted allele. (*C*) Northern blot analysis of *PINK1* transcripts. The blot is hybridized with a probe specific for exon 8, followed by hybridization of a probe specific for *GAPDH* cDNA as control. (*D*) Normal morphology of dopaminergic neurons in *PINK1*$^{-/-}$ mice is indicated by similar TH immunoreactivity in the SNpc of *PINK1*$^{-/-}$ mice and wilt-type controls at the age of 2–3 months. (*E*) Similar numbers of TH-positive neurons are present in the SNpc of *PINK1*$^{-/-}$ and wild-type mice at the ages of 2–3 months (+/+: 13,660 ± 1,033; −/−: 12,520 ± 573; $n = 4$ per genotype; $P > 0.05$) and 8–9 months (+/+: 13,547 ± 1,638; −/−: 14,446 ± 1,150; $n = 6$–7; $P > 0.05$). (*F*) Similar striatal content of DA in *PINK1*$^{-/-}$ mice and wild-type controls at the ages of 2–3 months (+/+: 14.3 ± 0.7; −/−: 13.2 ± 1.8; $n = 5$ per genotype; $P > 0.05$) and 8–9 months (+/+: 15.8 ± 0.9, −/−: 17.7 ± 2.3; $n = 5$–7 per genotype; $P > 0.05$).

degraded (Fig. 1*C*). We therefore concluded that germ-line deletion of exons 4–7 results in a *PINK1*-null allele, and that the homozygous mutant mice recapitulate the loss-of-function mutations in *PINK1*-linked PD.

Numbers of Dopaminergic Neurons and Levels of Striatal Dopamine (DA) Are Normal in *PINK1*$^{-/-}$ Mice. Because selective neurodegeneration occurs predominantly in the nigrostriatal dopaminergic system of PD patients, we examined coronal brain sections through the striatum and substantia nigra of *PINK1*$^{-/-}$ mice and wild-type controls. Immunohistochemical analysis using antibodies specific for tyrosine hydroxylase (TH) showed no gross abnormality in morphology and density of dopaminergic cell bodies (Fig. 1*D*) or dopaminergic projections to the striatum (data not shown) in *PINK1*$^{-/-}$ mice. Stereological counting of TH-immunoreactive neurons revealed unaltered numbers of dopaminergic neurons in the SNpc of *PINK1*$^{-/-}$ mice at the ages of 2–3 ($n = 4$, $P > 0.05$) and 8–9 months ($n = 6$–7, $P > 0.05$; Fig. 1*E*).

To determine whether loss of PINK1 function affects DA levels in the striatum, we used reverse phase HPLC to measure total amounts of DA and its major metabolites, dihydroxyphenylacetic acid (DOPAC) and homovanillic acid (HVA), in striata dissected from *PINK1*$^{-/-}$ and control mice. Levels of DA (Fig. 1*F*), DOPAC, and HVA (data not shown) are not significantly altered in the striatum of *PINK1*$^{-/-}$ mice ($n = 5$–9 per genotype; $P > 0.05$) at the ages of 2–3 and 8–9 months, suggesting normal DA synthesis and turnover in the absence of PINK1. Because TH is a rate-limiting enzyme in DA synthesis, we also measured levels of *TH* mRNA and protein. Real-time RT-PCR and Western blot analyses showed unchanged levels of *TH* mRNA and protein in *PINK1*$^{-/-}$ brains, respectively. We further measured TH activity *in vivo* through quantification of the TH product, L-DOPA, by HPLC in the presence of NSD-1015, an inhibitor of the aromatic L-amino acid DOPA decarboxylase, which can pass the blood–brain barrier and blocks the conversion of L-DOPA to DA. Levels of L-DOPA in the dissected striatum are unchanged in *PINK1*$^{-/-}$ mice (+/+: 0.61 ± 0.03, −/−: 0.62 ± 0.03, $n = 5$ per genotype), suggesting normal TH activity in the absence of PINK1.

Evoked Release of DA and Catecholamine Is Reduced in *PINK1*$^{-/-}$ Mice. To examine further the role of PINK1 in the dopaminergic system, we performed amperometric recordings by using acute striatal slices of *PINK1*$^{-/-}$ and wild-type mice at the age of 2–3 months. Slices from wild-type mice showed a mean evoked DA signal of $26.0 \pm 2.3 \times 10^6$ molecules ($n = 117$ stimulations in 25 slices from 10 mice), whereas *PINK1*$^{-/-}$ slices averaged $18.5 \pm 2.7 \times 10^6$ molecules ($n = 102$ stimulations in 23 slices from 10 mice; *, $P < 0.05$), indicating a significant decrease in evoked DA overflow in *PINK1*$^{-/-}$ mice (Fig. 2*A*). Because evoked DA overflow is determined essentially by DA release and reuptake, which is mediated through the DA transporter, we measured evoked DA overflow in the presence of the DA reuptake blocker nomifensine to determine whether reduced DA overflow was caused by decreased DA release and/or increased DA reuptake, and found that *PINK1*$^{-/-}$ slices showed a decrease in mean evoked DA signal ($24.4 \pm 3.5 \times 10^6$ molecules, $n = 39$ stimulations in 8 slices from 6 mice), compared with wild-type mice ($60.4 \pm 6.4 \times 10^6$ molecules, $n = 105$ stimulations in 21 slices from 8 mice; **, $P < 0.01$; Fig. 2*A*). These results demonstrate that PINK1 inactivation causes a marked decrease in evoked DA release.

To characterize further the effects of PINK1 inactivation on catecholamine release, we performed amperometric recordings on dissociated adrenal chromaffin cells, which are excellent models for the study of catecholamine release, because they permit the resolution of a single quantum released from dense core vesicles (16). We measured evoked catecholamine release from chromaffin cells derived from *PINK1*$^{-/-}$ and wild-type mice (Fig. 2*B*). Total catecholamine release per cell during the 6-second stimulation is much lower in *PINK1*$^{-/-}$ cells (+/+: $50.2 \pm 5.03 \times 10^6$; −/−: $25.0 \pm 2.48 \times 10^6$; **, $P < 0.01$; Fig. 2*B*). Mean catecholamine quantal size in *PINK1*$^{-/-}$ cells ($52.4 \pm 2.7 \times 10^4$ molecules, 4,465 vesicles from 100 cells) is smaller than that in wild-type controls ($77.6 \pm 3.9 \times 10^4$ molecules, 6,381 vesicles from 110 cells, *, $P < 0.01$; Fig. 2*B*). Furthermore, mean interspike interval in *PINK1*$^{-/-}$ cells (2.1 ± 0.3 seconds) is greater compared with controls (1.3 ± 0.1 seconds, **, $P < 0.01$; Fig. 2*B*), indicating a reduction in frequency of quantal release in the absence of PINK1. These results provide further support for a decrease in catecholamine release in *PINK1*$^{-/-}$ mice.

Corticostriatal Long-Term Potentiation (LTP) Impairment Can Be Reversed by D1 Receptor Agonists. Because DA modulates corticostriatal glutamatergic neurotransmission at medium-sized spiny (MS) neurons in the striatum, we performed electrophysiological recordings of MS neurons to determine the consequence of decreased synaptic release of DA. Whole-cell recordings of MS neurons from acute corticostriatal slices showed normal properties (e.g., resting membrane potential, input resistance) in

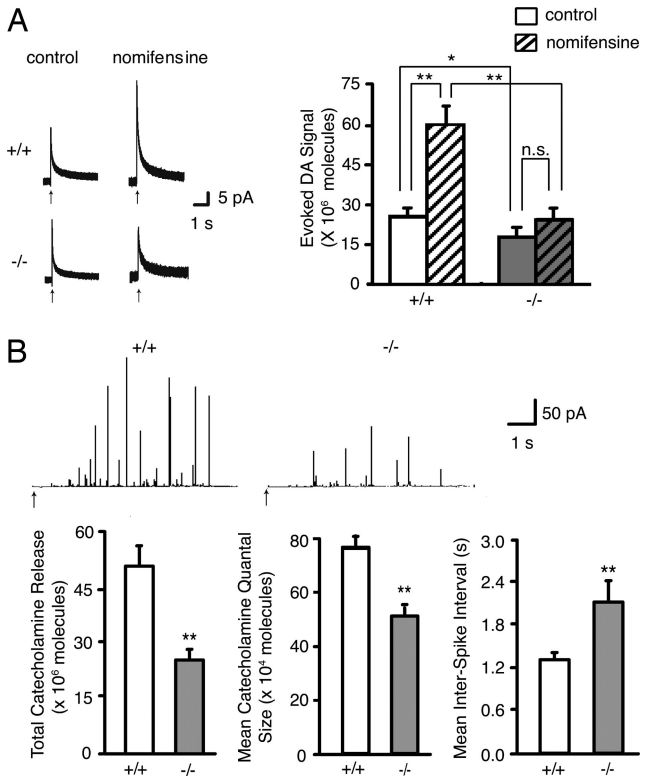

Fig. 2. Evoked release of catecholamine is decreased in *PINK1*$^{-/-}$ mice. (*A*) Reduction of evoked DA release in the *PINK1*$^{-/-}$ striatum. Representative amperometric traces of electrical stimulation-evoked DA release in the absence (control) and the presence of nomifensine are shown on the left. Arrows indicate the onset of electrical pulses. *PINK1*$^{+/+}$ slices show a mean evoked DA signal of 26.0 ± 2.3 × 10^6 molecules, whereas *PINK1*$^{-/-}$ slices show a lower evoked DA signal of 18.5 ± 2.7 × 10^6 molecules (*, $P < 0.05$), indicating a reduction in evoked DA overflow in *PINK1*$^{-/-}$ mice. In the presence of nomifensine, the mean evoked DA signal in *PINK1*$^{+/+}$ striatal slices but not in *PINK1*$^{-/-}$ striatal slices is significantly increased (60.4 ± 6.4 × 10^6 molecules) compared with the control condition without nomifensine (26.0 ± 2.3 × 10^6 molecules; **, $P < 0.01$). Data in all panels are expressed as mean ± SEM. (*B*) Reduction of evoked catecholamine release in *PINK1*$^{-/-}$ chromaffin cells. Amperometric traces of 80 mM K^+-evoked catecholamine release are shown at the top. Arrows mark the onset of high K^+ stimulation. Total catecholamine release per cell during the 6-second stimulation is much lower in *PINK1*$^{-/-}$ mice (25.0 ± 2.5 × 10^6) compared with wild-type controls (50.2 ± 5.0 × 10^6; **, $P < 0.01$). The mean catecholamine quantal size is also reduced in *PINK1*$^{-/-}$ chromaffin cells (52.4 ± 2.6 × 10^4 compared with *PINK1*$^{+/+}$ cells (77.6 ± 3.9 × 10^4; **, $P < 0.01$). Frequency of quantal release is significantly lower in *PINK1*$^{-/-}$ cells, as indicated by a lower mean interspike interval in *PINK1*$^{+/+}$ (1.3 ± 0.1) than in *PINK1*$^{-/-}$ cells (2.1 ± 0.3; **, $P < 0.01$). Data in all panels are expressed as mean ± SEM.

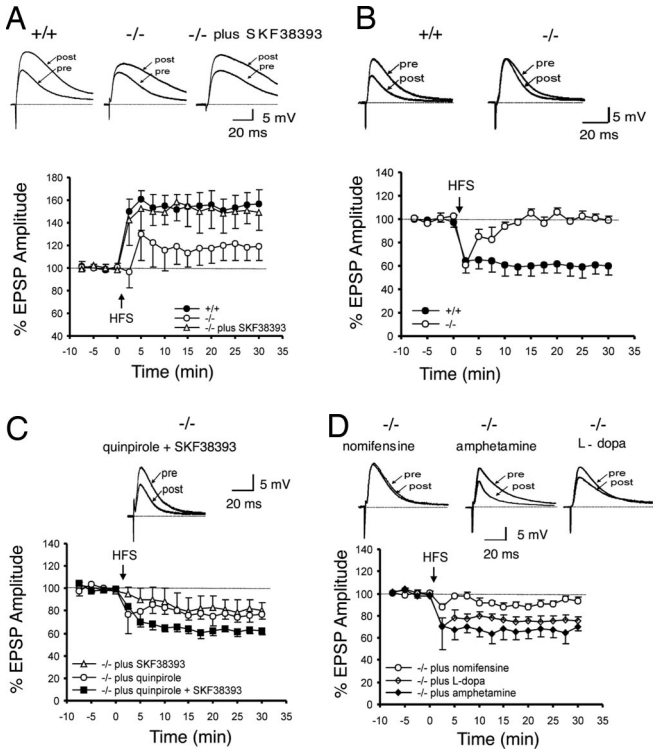

Fig. 3. Reversal of synaptic plasticity impairment by DA receptor agonists or agents increasing DA release in *PINK1*$^{-/-}$ mice. (*A*) Corticostriatal LTP induced by HFS in the absence of Mg^{2+} in *PINK1*$^{-/-}$ MS neurons is lower than in controls. Preincubation with the D1 receptor agonist SKF 38393 restores LTP to the level obtained in controls. (*B*) Corticostriatal LTD induced by HFS in the presence of Mg^{2+} is absent in *PINK1*$^{-/-}$ MS neurons. (*C*) Coadministration of D1 (SKF38393) and D2 receptor (quinpirole) agonists fully restores LTD in *PINK1*$^{-/-}$ neurons, whereas application of SKF38393 or quinpirole alone partially rescues LTD impairment. (*D*) Preincubation with nomifensine does not rescue LTD deficits, whereas pretreatment with amphetamine rescues the LTD impairment completely. L-dopa is able to restore, to a significant extent, the striatal LTD deficit. Each data point represents the mean ± SEM of at least four independent observations. In each panel, the superimposed traces representing the EPSPs recorded before (pre) and 20 min after (post) tetanic stimulation are shown above.

PINK1$^{-/-}$ mice. Upon depolarizing current pulses, membrane rectification and tonic action potential discharges are similar between *PINK1*$^{-/-}$ and wild-type mice (n = 18–27 neurons; $P > 0.05$). To look for possible alterations in glutamate release probability or short-term plasticity, we performed intracellular recordings of MS neurons to measure spontaneous excitatory postsynaptic currents (sEPSCs) and miniature EPSCs (mEPSCs). In the presence of bicuculline, the frequency and amplitude of glutamate-dependent sEPSCs are normal in *PINK1*$^{-/-}$ MS neurons (n = 19–22; $P > 0.05$). Similarly, both frequency and amplitude of mEPSCs, recorded in the presence of bicuculline and tetrodotoxin, are also normal in the absence of PINK1 (n = 10–13 neurons; $P > 0.05$). Furthermore, paired-pulse ratio (PPR), an indicator of modified presynaptic release (17), is unchanged in *PINK1*$^{-/-}$ MS neurons (n = 13–14; $P > 0.05$).

We then performed intracellular recordings to measure LTP at corticostriatal synapses. LTP induced by high-frequency stimulation (HFS) in the absence of magnesium in *PINK1*$^{-/-}$ MS neurons (117.1 ± 12.7%; n = 4) is lower than that from wild-type controls (156.0 ± 12.0%; n = 8, $P < 0.05$; Fig. 3*A*). Because corticostriatal LTP induction depends on activation of D1 type DA receptors (18, 19), we examined whether D1 receptor-like agonists can reverse this LTP defect in *PINK1*$^{-/-}$ mice. Indeed, preincubation of corticostriatal slices with a D1 receptor agonist, SKF 38393, restored LTP fully (153 ± 18.3%; n = 4; Fig. 3*A*).

To test whether the observed synaptic plasticity impairment is specific for corticostriatal glutamatergic synapses, which receive modulatory dopaminergic inputs from the SNpc, we measured synaptic transmission and plasticity at another glutamatergic synapse, the Schaeffer collateral pathway of the hippocampus, in *PINK1*$^{-/-}$ mice. Input/output (I/O) curves are similar in *PINK1*$^{-/-}$ and control mice ($P > 0.8$), indicating normal basal synaptic transmission [supporting information (SI) Fig. 5*A*; see also *SI Materials and Methods*]. LTP induced by five trains of θ-burst stimulation (TBS) is unaffected in *PINK1*$^{-/-}$ mice (SI Fig. 5*B*). The magnitude of LTP measured 60 min after induction is similar in *PINK1*$^{-/-}$ (155.4 ± 6.2%) and control mice (156.9 ± 6.8%, P = 0.48). These results show that PINK1

inactivation does not alter normal synaptic plasticity in a hippocampal glutamatergic synapse.

Corticostriatal Long-Term Depression (LTD) Impairment Can Be Restored by DA Receptor Agonists or Agents Increasing DA Release. In the presence of magnesium, HFS of cortical afferents induces LTD of corticostriatal EPSPs in wild-type MS neurons (62 ± 8.4%, measured 20 min after HFS, $n = 10$; Fig. 3*B*). LTD induction in *PINK1*$^{-/-}$ MS neurons, however, is absent (106 ± 4%, $n = 7$; Fig. 3*B*). Because LTD induction depends on activation of both D1 and D2 receptors (20), we tried to restore LTD induction with either D1 and D2 agonists alone or both D1 and D2 agonists. Pretreatment of corticostriatal slices with either the D1-like receptor agonist SKF38393 (83 ± 10%) or the D2-like receptor agonist quinpirole (75.2 ± 8.8%) partially restored LTD induction in *PINK1*$^{-/-}$ neurons ($n = 7$; Fig. 3*C*). The use of both agonists, SKF38393 and quinpirole, restored LTD to control levels (62 ± 4%, $n = 5$; Fig. 3*C*).

The fact that the synaptic plasticity deficits in *PINK1*$^{-/-}$ mice can be rescued by D1 and D2 receptor agonists prompted us to examine whether loss of PINK1 reduces densities of striatal D1 and D2 receptors. Radioligand binding autoradiography has previously been used to demonstrate the abundance of D1 and D2 receptors in the striatum, as shown by high levels of binding to radioactively labeled antagonists of D1- ([^{3}H]SCH23390) and D2- ([^{3}H]spiperone) like receptors and by the disappearance of the binding signals in the striatum of the respective knockout mice (21–23). We therefore performed radioligand binding assays to measure levels of surface D1 and D2 receptors by using [^{3}H]SCH23390 and [^{3}H]spiperone (SI Fig. 6*A*; see also *SI Materials and Methods*). Quantitative analysis of binding densities in the striatum revealed no significant difference in the density of D1 and D2 receptors between the genotypic groups, indicating normal levels of surface D1 and D2 receptors in the *PINK1*$^{-/-}$ striatum (SI Fig. 6*B*).

The reversal of LTD deficits by D1 and D2 agonists and the absence of decreases in the levels of D1 and D2 receptors suggest that D1 and D2 signaling are still functional in *PINK1*$^{-/-}$ mice. Thus, the striatal synaptic plasticity impairment is likely caused by reduced synaptic release of DA in *PINK1*$^{-/-}$ mice. To investigate this further, we explored how agents that affect DA release would affect corticostriatal synaptic plasticity. We first tested the effect of amphetamine, which causes increases of DA in the synaptic cleft. Interestingly, in the presence of amphetamine, we indeed observed a complete rescue of striatal LTD in *PINK1*$^{-/-}$ slices (66.4 ± 7.2%, $n = 4$ neurons; Fig. 3*D*). The finding that amphetamine, which increases DA release, rescues LTD deficits in *PINK1*$^{-/-}$ slices provides direct supporting evidence for reduction of evoked DA overflow as the mechanism underlying LTD deficits observed in *PINK1*$^{-/-}$ mice. We also examined the effect of nomifensine, which failed to increase evoked DA overflow in *PINK1*$^{-/-}$ mice (Fig. 2*A*), on LTD induction, and found that nomifensine did not restore LTD induction significantly (90.0 ± 2.5%, $n = 4$; Fig. 3*D*). Lastly, pretreatment of slices with DA precursor L-dopa, which increases DA production and thus the amount of DA available for release upon stimulation, rescued striatal LTD induction in *PINK1*$^{-/-}$ neurons (74.4 ± 4.7%, $n = 5$; Fig. 3*D*). These results provide further support for the impairment in evoked DA release as the likely mechanism underlying the striatal synaptic plasticity deficits observed in *PINK1*$^{-/-}$ mice.

Discussion

To gain insight into the pathogenic mechanism by which *PINK1* deficiency causes PD, we use a genetic approach to explore the normal function of PINK1 in the nigrostriatal pathway, a neural circuit that is particularly vulnerable in PD. Our results reveal an essential and selective role for PINK1 in dopaminergic synaptic transmission (Fig. 4). Specifically, we found that PINK1 inactivation impairs DA release but does not alter levels of DA, numbers of dopaminergic neurons, DA synthesis or levels of DA receptors. The impairment in DA release in *PINK1*$^{-/-}$ mice is sufficient to compromise nigrostriatal circuit function, as indicated by the deficits in corticostriatal bidirectional synaptic plasticity, which could be restored by agents that either increase presynaptic DA release (amphetamine and L-dopa) or activate postsynaptic DA receptor function directly (D1 and D2 receptor agonists).

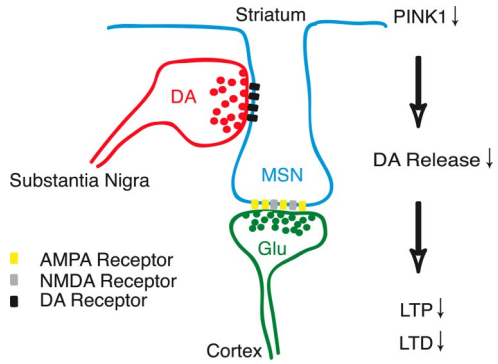

Fig. 4. A schematic model for PINK1 function at the nigrostriatal and corticostriatal heterosynapse. This schematic model illustrates the neuromodulatory role of the nigrostriatal input at glutamatergic corticostriatal synapses of striatal medium spiny neurons (MSN). Coincident activation of convergent nigrostriatal dopaminergic and corticostriatal glutamergic inputs elicits synaptic release of DA and glutamate and activation of postsynaptic D1/D2 and NMDA/AMPA receptors, respectively. Activation of D1 receptors is necessary for the induction of LTP at corticostriatal synapses, whereas activation of both D1 and D2 receptors is necessary for induction of LTD. In the absence of PINK1, impaired release of DA from nigrostriatal terminals leads to reduced activation of postsynaptic D1 and D2 receptors, and consequent defects in both LTP and LTD.

PINK1 Plays an Essential Role in Presynaptic DA Release and Corticostriatal Synaptic Plasticity. Several lines of evidence support the conclusion that loss of PINK1 function causes a selective impairment in DA release. Amperometric recordings in acute striatal slices demonstrated a reduction in evoked DA overflow in *PINK1*$^{-/-}$ mice (Fig. 2). Evoked DA overflow, which is measured as evoked DA signals, reflects the balance of electrically stimulated DA release and reuptake, and altered DA signals could, in principle, arise through changes in either process. As expected, the DA reuptake inhibitor nomifensine greatly enhanced the evoked DA signal in the control striatum. In contrast, blockade of DA reuptake had little effect on the DA signal in the *PINK1*$^{-/-}$ striatum. Together, these results demonstrate that the reduction of evoked DA overflow in *PINK1*$^{-/-}$ mice is caused by a decrease in exocytotic DA release rather than an increase in reuptake. Studies of evoked catecholamine release in chromaffin cells provided further support for a defect in exocytotic DA release, as indicated by significant reductions in the total catecholamine release, quantal size and release frequency in *PINK1*$^{-/-}$ mice (Fig. 2). Impaired DA release in *PINK1*$^{-/-}$ mice is not attributable to alterations in DA synthesis or in numbers of dopaminergic neurons in *PINK1*$^{-/-}$ mice (Fig. 1), further indicating that the impaired DA release reflects a functional rather than structural defect.

DA release from nigrostriatal projections modulates excitatory corticostriatal synaptic transmission and plasticity (Fig. 4). Our functional analysis of the nigrostriatal circuit in *PINK1*$^{-/-}$ mice disclosed a marked impairment of bidirectional striatal synaptic plasticity (Fig. 3). In the absence of PINK1, induction of LTP and LTD is impaired at corticostriatal synapses, the

major target of nigrostriatal dopaminergic inputs. Corticostriatal LTP induction depends on activation of D1 receptors, whereas LTD induction depends on activation of both D1 and D2 receptors (18, 24). Thus, the observed impairments in LTP and LTD are consistent with either a reduction in presynaptic DA release or a deficiency in postsynaptic D1 and D2 receptor-mediated functions. In agreement with the finding that DA release is reduced in *PINK1*$^{-/-}$ mice, we observed that DA receptor agonists potently rescued the impairments in LTP and LTD in *PINK1*$^{-/-}$ mice. This observation suggests that direct activation of appropriate postsynaptic DA receptors compensates for a presynaptic defect in DA release.

Full rescue of LTP and LTD deficits in *PINK1*$^{-/-}$ mice by the appropriate agonists indicates that postsynaptic D1 and D2 receptor function remains intact, consistent with the normal levels of striatal D1 and D2 receptors observed by radioligand binding autoradiography (SI Fig. 6). Moreover, intrinsic physiologic properties of MS neurons are normal, as are glutamatergic synaptic transmission and short-term plasticity, providing further evidence against postsynaptic or glutamatergic dysfunction. Furthermore, glutamatergic synaptic transmission and LTP in the Schaeffer collateral pathway of the hippocampus are normal (SI Fig. 5), arguing against a generalized glutamatergic defect. Thus, the observed deficits in corticostriatal LTP and LTD are most compatible with a specific defect in presynaptic dopaminergic function.

How does PINK1 function in the regulation of exocytotic DA release? Studies of PINK1 so far have suggested that PINK1 may function as a mitochondrial kinase (3, 25). *PINK1*$^{-/-}$ flies indeed exhibit striking mitochondrial morphological defects (26, 27). However, we did not observe overt mitochondrial morphological defects in *PINK1*$^{-/-}$ mice (T.K. and J.S., unpublished results), perhaps because of better compensatory mechanisms and greater genetic redundancies in mice compared with *Drosophila*, although it remains possible that subtle mitochondrial defects exist in *PINK1*$^{-/-}$ mice. Although little is known about the mechanisms of exocytotic DA release, it likely uses a similar mechanism as glutamatergic synapses, in which release is energy-dependent, is mediated by the SNARE-dependent fusion of synaptic vesicles, and is triggered by Ca^{2+} binding to synaptotagmins (28). If PINK1 is indeed a mitochondrial kinase, our results would suggest a possible functional link between mitochondria and the regulation of DA exocytosis.

Implications for PD Pathogenesis. The pathophysiological hallmark of parkinsonian syndromes is reduced dopaminergic input to the striatum. PET and SPECT studies of PD patients carrying heterozygous or homozygous PINK1 mutations have suggested presynaptic dopaminergic defects and loss of dopaminergic terminals in the striatum (13–15). Similar to our prior findings in *parkin*$^{-/-}$ (29) and *DJ-1*$^{-/-}$ mice (30), *PINK1*$^{-/-}$ mice do not exhibit evidence of nigrostriatal neurodegeneration, at least not by the age of 9 months (Fig. 1). Although it remains possible that *PINK1*$^{-/-}$ mice may develop nigral degeneration at an older age, this possibility is unlikely, given that *parkin*$^{-/-}$ (29) and *DJ-1*$^{-/-}$ (H.Y. and J.S., unpublished results) mice fail to develop significant dopaminergic neurodegeneration at the age of 24 months. Nevertheless, the reduced release of DA by nigrostriatal terminals in *PINK1*$^{-/-}$ mice closely parallels the functional consequences of dopaminergic denervation in PD. Further extending this analogy, L-dopa ameliorates functional deficits in the nigrostriatal pathway in *PINK1*$^{-/-}$ mice (Fig. 3) and clinical symptoms in PD patients. We therefore propose that impaired presynaptic release of DA may be a common pathophysiologic mechanism in PD, possibly representing a mechanistic precursor within a spectrum of nigrostriatal dysfunction leading to frank neurodegeneration.

Several additional lines of evidence support this presynaptic hypothesis. First, amphetamine-induced hyperactivity in the open field is reduced in both *parkin*$^{-/-}$ (31) and *DJ-1*$^{-/-}$ mice (32), suggesting a common defect in amphetamine-induced DA release. Second, we previously reported that evoked DA overflow is reduced in acute striatal slices of *DJ-1*$^{-/-}$ mice (30). Third, we recently obtained similar evidence for reduced DA release from nigrostriatal terminals in *parkin*-deficient mice from amperometric recordings of both acute striatal slices and dissociated chromaffin cells (T.K., E.N.P., and J.S., unpublished results). This functional convergence on the regulation of exocytotic DA release among parkin, DJ-1 and PINK1 suggests a common pathophysiologic mechanism in recessive parkinsonism, a hypothesis that could also explain the functional redundancy observed between *Drosophila* parkin and PINK1 (26, 27). How presynaptic defects and decreased DA release may compromise the survival of dopaminergic neurons awaits future studies to understand the mechanism by which a chronic deficiency in DA release could lead to gradual loss of dopaminergic terminals and ultimately cell bodies.

Methods

Generation of *PINK1*$^{-/-}$ Mice. The targeting vector was generated by using the 1.9-kb DNA fragment (KpnI–Bsr GI) from a *PINK1* BAC clone (Invitrogen, Carlsbad, CA) as the 5′ homologous region. The 2.1-kb DNA fragment amplified by PCR using primers 1 and 2 was used as the 3′ homologous region. The targeting vector also includes a positive *PGK-Neo* selection cassette and a negative *PGK-DT* selection cassette. The linearized targeting vector was transfected into both J1 (129/Sv) and MK (129/Sv; C57BL/6 F1 hybrid) ES cells by using standard procedures. Two ES clones (MK and J1) were injected into blastocytes of C57BL/6 or Balb C mice. Chimeric mice obtained from ES clone 1 (MK) were intercrossed with 129/Sv;C57BL/6 F_1 hybrid mice to acquire F_1 heterozygous mutant mice, which were then intercrossed to obtain homozygous mutant mice for further analysis. All experiments except the molecular analysis were performed in a genotype-blind manner.

Histology and Neuron Counting. Four pairs of brains from both genotypic groups were embedded in each paraffin block and sectioned at 16-μm thickness. Immunohistochemical analysis for TH (1:1,000, rabbit anti-TH; Chemicon, Temecula, CA) and Nissl counterstain were carried out by using Vector Elite ABC kit with DAB on every 10th midbrain sections throughout the entire SN. The number of DA neurons in the SN was determined by counting TH-immunoreactive neurons in coronal sections by using the fractionator and optical dissector methods of unbiased stereology, an image analyzing system controlled by a computer equipped with a BX51 microscope (Olympus, Melville, NY), CCD camera, and Bioquant image analysis software.

Amperometric Recordings. Preparation of acute coronal striatal slices and use of carbon fiber microelectrodes and electrical stimulation parameters were previously described in (30). Local bath application of the DA reuptake blocker nomifensine (3 μM) for 30 min was used to assess the contribution of reuptake in the evoked DA signal. For preparation of dissociated adrenal chromaffin cells, dissected medullae were dissociated with Ca^{2+}-free collagenase IA solution (0.2%) for 30 min and triturated in 1% BSA and 0.02% DNase. The cell culture medium contained DMEM, 10% FBS, 50 units/ml penicillin, and 50 μg/ml streptomycin. The cell suspension was placed onto laminin-coated glass wells in 35-mm dishes. Cells were maintained in a 5% CO_2 incubator at 37°C. Amperometric recordings took place between days 1 and 3 after plating with carbon fiber microelectrodes (5-μm tip diameter) after picospritzing an 80 mM K^+ solution for 6 sec on individual cells. Data acquisition occurred at 50 kHz and was digitally postfiltered at 1 kHz. Statistical significance was analyzed through one-way ANOVA of the means for quantal size, amplitude, width, and interspike interval.

Electrophysiology. Corticostriatal slices (≈250 μm) were prepared from mice at the age of 2–3 months as described (30). Whole-cell recordings were performed from individual neurons visualized with differential interference contrast and infrared microscopy. Pipettes (3–5 MΩ) were filled with an internal solution containing 125 mM K^+-gluconate, 10 mM NaCl, 1 mM $CaCl_2$, 2 mM $MgCl_2$, 1 mM BAPTA, 19 mM Hepes, 0.3 mM GTP, and 2 mM Mg-ATP, adjusted to pH 7.3 with KOH. Signals were amplified with Axopatch 200B and stored on PC (Digidata 1200 and pClamp9). Current-voltage (I–V) relationship was assessed by voltage-clamp experiments (holding potential −80 mV), applying 10-mV steps (0.3 s) from −140 to −40 mV. A negative step (−10 mV) was used to measure membrane resistance. Firing properties were investigated in current-clamp mode applying 200 pA steps (1 s) from −500 to +700 pA. For sEPSCs, 10 μM bicuculline was added to block $GABA_A$-mediated transmission. To isolate mEPSCs, we applied tetrodotoxin (TTX, 1 μM). EPSCs were recorded and analyzed offline (MiniAnalysis 6.1; Synaptosoft).

Corticostriatal EPSPs were evoked with a bipolar electrode placed in the white matter. Test stimuli were delivered at 0.1 Hz in bicuculline. For HFS, (three trains: 3-sec duration, 100 Hz frequency, 20-sec intervals), stimulus intensity was raised to suprathreshold levels. Mg^{2+} was omitted from the solution to induce LTP. For each cell, the amplitude of six EPSPs was averaged and plotted as a percentage of the amplitude averaged for a period of ≈10 min pre-HFS. For paired-pulse recordings, we measured the EPSP2/EPSP1 ratio (PPR, 50-ms interstimulus interval). Values given are mean ± SEM. Student's *t* test was used to assess statistical significance. Drugs (bicuculline-methiodide; Sigma, St. Louis, MO; SKF38398, quinpirole; Tocris, Ellisville, MO) were applied by switching the control perfusion to drug-containing solution.

We thank Matthew Goldberg, Laura Corina, Franco Lavaroni, Massimo Tolu, and Lan Wang for assistance. This work was supported by grants from the National Institute of Neurological Disorders and Stroke and the Michael J. Fox Foundation (to J.S.), the Parkinson's Disease Foundation (T.K., E.N.P.), Ministero dell' Instruzione, dell'Università e della Ricerca (Italian Fund for Basic Research), Ministero Salute Progetto Finalizzato and Agenzia Spaziale Italiana (A.P.).

1. Kitada T, Asakawa S, Hattori N, Matsumine H, Yamamura Y, Minoshima S, Yokochi M, Mizuno Y, Shimizu N (1998) *Nature* 392:605–608.
2. Bonifati V, Rizzu P, van Baren MJ, Schaap O, Breedveld GJ, Krieger E, Dekker MC, Squitieri F, Ibanez P, Joosse M, *et al.* (2003) *Science* 299:256–259.
3. Valente EM, Abou-Sleiman PM, Caputo V, Muqit MM, Harvey K, Gispert S, Ali Z, Del Turco D, Bentivoglio AR, Healy DG, *et al.* (2004) *Science* 304:1158–1160.
4. Unoki M, Nakamura Y (2001) *Oncogene* 20:4457–4465.
5. Rohe CF, Montagna P, Breedveld G, Cortelli P, Oostra BA, Bonifati V (2004) *Ann Neurol* 56:427–431.
6. Hatano Y, Li Y, Sato K, Asakawa S, Yamamura Y, Tomiyama H, Yoshino H, Asahina M, Kobayashi S, Hassin-Baer S, *et al.* (2004) *Ann Neurol* 56:424–427.
7. Valente EM, Salvi S, Ialongo T, Marongiu R, Elia AE, Caputo V, Romito L, Albanese A, Dallapiccola B, Bentivoglio AR (2004) *Ann Neurol* 56:336–341.
8. Healy DG, Abou-Sleiman PM, Gibson JM, Ross OA, Jain S, Gandhi S, Gosal D, Muqit MM, Wood NW, Lynch T (2004) *Neurology* 63:1486–1488.
9. Bonifati V, Rohe CF, Breedveld GJ, Fabrizio E, De Mari M, Tassorelli C, Tavella A, Marconi R, Nicholl DJ, Chien HF, *et al.* (2005) *Neurology* 65:87–95.
10. Ibanez P, Lesage S, Lohmann E, Thobois S, De Michele G, Borg M, Agid Y, Durr A, Brice A (2006) *Brain* 129:686–694.
11. Hedrich K, Hagenah J, Djarmati A, Hiller A, Lohnau T, Lasek K, Grunewald A, Hilker R, Steinlechner S, Boston H, *et al.* (2006) *Arch Neurol* 63:833–838.
12. Valente EM, Brancati F, Ferraris A, Graham EA, Davis MB, Breteler MM, Gasser T, Bonifati V, Bentivoglio AR, De Michele G, *et al.* (2002) *Ann Neurol* 51:14–18.
13. Khan NL, Valente EM, Bentivoglio AR, Wood NW, Albanese A, Brooks DJ, Piccini P (2002) *Ann Neurol* 52:849–853.
14. Kessler KR, Hamscho N, Morales B, Menzel C, Barrero F, Vives F, Gispert S, Auburger G (2005) *J Neural Transm* 112:1345–1353.
15. Albanese A, Valente EM, Romito LM, Bellacchio E, Elia AE, Dallapiccola B (2005) *Neurology* 64:1958–1960.
16. Albillos A, Dernick G, Horstmann H, Almers W, Alvarez de Toledo G, Lindau M (1997) *Nature* 389:509–512.
17. Schulz PE, Cook EP, Johnston D (1994) *J Neurosci* 14:5325–5337.
18. Centonze D, Picconi B, Gubellini P, Bernardi G, Calabresi P (2001) *Eur J Neurosci* 13:1071–1077.
19. Kerr JN, Wickens JR (2001) *J Neurophysiol* 85:117–124.
20. Calabresi P, Maj R, Pisani A, Mercuri NB, Bernardi G (1992) *J Neurosci* 12:4224–4233.
21. Xu M, Moratalla R, Gold LH, Hiroi N, Koob GF, Graybiel AM, Tonegawa S (1994) *Cell* 79:729–742.
22. Yamaguchi H, Aiba A, Nakamura K, Nakao K, Sakagami H, Goto K, Kondo H, Katsuki M (1996) *Genes Cells* 1:253–268.
23. Thanos PK, Taintor NB, Alexoff D, Vaska P, Logan J, Grandy DK, Fang Y, Lee JH, Fowler JS, Volkow ND, *et al.* (2002) *J Nucl Med* 43:1570–1577.
24. Gubellini P, Pisani A, Centonze D, Bernardi G, Calabresi P (2004) *Prog Neurobiol* 74:271–300.
25. Silvestri L, Caputo V, Bellacchio E, Atorino L, Dallapiccola B, Valente EM, Casari G (2005) *Hum Mol Genet* 14:3477–3492.
26. Clark IE, Dodson MW, Jiang C, Cao JH, Huh JR, Seol JH, Yoo SJ, Hay BA, Guo M (2006) *Nature* 441:1162–1166.
27. Park J, Lee SB, Lee S, Kim Y, Song S, Kim S, Bae E, Kim J, Shong M, Kim JM, *et al.* (2006) *Nature* 441:1157–1161.
28. Südhof TC (2004) *Annu Rev Neurosci* 27:509–547.
29. Goldberg MS, Fleming SM, Palacino JJ, Cepeda C, Lam HA, Bhatnagar A, Meloni EG, Wu N, Ackerson LC, Klapstein GJ, *et al.* (2003) *J Biol Chem* 278:43628–43635.
30. Goldberg MS, Pisani A, Haburcak M, Vortherms TA, Kitada T, Costa C, Tong Y, Martella G, Tscherter A, Martins A, *et al.* (2005) *Neuron* 45:489–496.
31. Itier JM, Ibanez P, Mena MA, Abbas N, Cohen-Salmon C, Bohme GA, Laville M, Pratt J, Corti O, Pradier L, *et al.* (2003) *Hum Mol Genet* 12:2277–2291.
32. Kim RH, Smith PD, Aleyasin H, Hayley S, Mount MP, Pownall S, Wakeham A, You-Ten AJ, Kalia SK, Horne P, *et al.* (2005) *Proc Natl Acad Sci USA* 102:5215–5220.